Heterogeneous & Homogeneous & Bio- & Nano-

CHEMCATCHEM

CATALYSIS

Accepted Article

Title: Catalytic conversion of CO2 to value-added products under mild conditions

Authors: Yuan Wang, Yulv Yu, and Jin Huang

To be cited as: *ChemCatChem* 10.1002/cctc.201801346

Link to VoR: http://dx.doi.org/10.1002/cctc.201801346

A Journal of ChemPubSoc Europe

WILEY-VCH

www.chemcatchem.org

Catalytic conversion of CO_2 to value-added products under mild conditions

*Yulv Yu, Jin Huang, Yuan Wang**

Abstract: *The catalytic synthesis of multi-carbon alcohols (MCA, $C_nH_{2n+1}OH$, n≥3) and higher hydrocarbons from CO_2 and H_2 under low or even ambient temperature are realized for the first time over a prepred bimetallic catalyst composed of nanoparticles of Pt and Ru supported on Fe_3O_4 (Ru-Pt/Fe_3O_4). At 40 ℃, the selectivity for alcohols, MCA, and higher hydrocarbons reached 77.1%, 4.5%, and 19.5%, respectively, while that for methane was only 3.4% (carbon based). As revealed by isotope tracer experiments using O^{18} labeled water, in the hydrogenation of CO_2 over Ru-Pt/Fe_3O_4, MCA could form by catalytic hydrolysis of alkyl, a novel reaction pathway enabling the formation of MCA at low temperature, which is different from the previously reported one based on CO insertion at high temperature. It was discovered that in Ru-Pt/Fe_3O_4, both Ru and Pt nanoparticles played catalytic roles in the reduction of CO_2 to CH_x species and the carbon-carbon coupling reaction to form alkyl, while the catalytic hydrolysis of formed long-chain alkyl occurred on Pt nanoparticles.*

CO_2 is a cheap, nontoxic, and abundant carbon source. The rising concentration of CO_2 in the atmosphere has been causing serious problems such as the greenhouse effect and ocean acidification. Therefore, the conversion of surplus CO_2 to hydrocarbon or oxygenated hydrocarbon is a significant subject [1-13]. The development of new catalytic systems capable of realizing the conversion of CO_2 to multi-carbon products (hydrocarbons or alcohols) at low or even ambient temperature is an attractive subject because such systems will not only provide high value products by consuming CO_2, but also avoid over-emission of CO_2 in the conversion process. MCA with 3-8 carbon atoms are not only liquid fuels but also widely used as fine chemicals or solvents in producing pharmaceuticals, polymers, surfactants, detergents, paints, and printing inks [14-16]. The conversion of CO_2 and H_2 to multi-carbon compounds (CCMC) should be an ideal CO_2 conversion route, and H_2 can be manufactured in a large scale from renewable energy sources, including solar energy, hydropower and biomass.

Pioneering efforts have been made to create catalytic systems for the conversion of CO_2 to multi-carbon compounds. It was reported that higher hydrocarbons could be synthesized from CO_2 and H_2 at high temperature over some heterogeneous catalysts. Song reported a Fe-Co bimetallic catalyst which could catalyze the reaction of CO_2 with H_2 to produce higher hydrocarbons with a selectivity of 69% and a small amount of MCA at 300 °C [17]. Recently, Ge and Sun prepared an efficient catalyst Na-Fe_3O_4/HZSM-5 which can catalyze hydrogenation of CO_2 to produce hydrocarbons containing 78% of gasoline-range (C_5-C_{11}) ones at a CO_2 conversion of 22% at 320 °C [18]. Sun et al. reported that a bifunctional catalyst composed of indium oxide (In_2O_3) and zeolites could catalyze the reaction of CO_2 with H_2 to produce gasoline-range hydrocarbons with a selectivity of 78.6% at 340 °C [19]. Chen and co-workers reported a composite catalyst CuZnFeK, over which hydrogenation of CO_2 under 6 MPa at 300 °C could produce alcohols and hydrocarbons with mass selectivities of 36.6 % and 56.4%, respectively, and the mass ratio of C_2^+ alcohols to C_1 alcohol was 6.76 [20]. We also noticed that Han and coworkers reported an interesting PtRu/Fe_2O_3 catalyst, prepared by reactions of a mixture of H_2PtCl_6, $RuCl_3$, and $Fe(NO_3)_3$ with $NaCO_3$, followed by reducing the obtained precipitate in hydrogen at 400 °C, which could catalyze hydrogenation of CO_2 at 200°C in DMI (1,3-dimethyl-2-imidazolidinone) to form C_2^+ alcohols with a selectivity of 36.0% (carbon based) [21]. Han et al. further found that at 200 °C, over a Pt/Co_3O_4 catalyst dispersed in a mixture of water and DMI, C_1-C_4 alcohols could be synthesized by hydrogenation of CO_2 with a selectivity of 33.1% (carbon based) [22]. Xiao et al. reported that over a cobalt catalyst ($CoAlO_x$) at 140 °C, ethanol could be produced with a selectivity as high as 92%, and a small amount of methanol, propanol, and butanol were also detected in the products [23]. However, to the best of our knowledge, catalysts which can realize the conversion of CO_2 and H_2 to multi-carbon products at ambient temperature have so far been scarce.

We have been engaging in the development of iron oxide or tin oxide supported metal nanocluster catalysts with metal nanoclusters stabilized with ethylene glycol and simple ions as building blocks for a long time [24-27]. In this paper, we report a novel heterogeneous catalyst composed of nanoparticles of Ru and Pt supported on Fe_3O_4 (Ru-Pt/Fe_3O_4), which could catalyze the conversion of CO_2 and H_2 to C_1-C_6 linear alcohols and C_1-C_6 light hydrocarbons at 40-60 °C, and C_1-C_8 alcohols and C_1-C_8 hydrocarbons at 80 °C.

The Ru-Pt/Fe_3O_4 catalyst was prepared by depositing Pt nanoclusters stabilized with ethylene glycol and simple ions [28] and Ru oxide nanoparticles [29] on a Fe_3O_4 support, consecutively, followed by reducing the obtained solid intermediate with 2.8 MPa of hydrogen in water at 150 °C (see the Experimental Section for details). The Pt and Ru contents of the prepared catalyst were measured by inductively coupled plasma atomic emission spectrometer (ICP-AES) to be 1.8 % and 3.6 %, respectively.

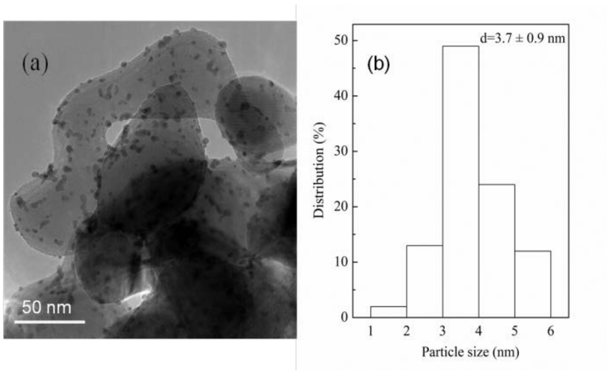

Figure 1. TEM image of Ru-Pt/Fe_3O_4 (a) and metal particle size distribution histogram (b).

As shown in the transmission electron microscope (TEM) image of Ru-Pt/Fe_3O_4 (Figure 1), metal nanoparticles dispersed on Fe_3O_4 had an average diameter of 3.7 nm, with a standard

---

Dr. Y. L. Yu, J. Huang, Prof. Y. Wang
Beijing National Laboratory for Molecular Sciences, State Key Lab for Structural Chemistry of Unstable and Stable Specie
College of Chemistry and Molecular Engineering, Peking University
Beijing 100871 (China)
E-mail: wangy@pku.edu.cn
Supporting information for this article is given via a link at the end of the document.

deviation of 0.9 nm, and aggregates of metal nanoparticles with sizes of ~10 nm also existed in the catalyst.

X-ray photoelectron spectroscopy (XPS) measurement on Ru-Pt/Fe_3O_4 (Figure 2) revealed that the binding energies of Ru $3p_{3/2}$ and Pt $4f_{7/2}$ levels were 462.6 eV and 71.2 eV, respectively, indicating that Ru and Pt were in metallic states.

The X-ray diffraction (XRD) pattern of Ru-Pt/Fe_3O_4 (Supporting Information Fig S1), exhibited diffraction peaks at 18.3, 30.1, 35.4, 37.1, 43.1, 53.4, 57.0, and 62.5° corresponding to the diffraction signals of (111), (220), (311), (222), (400), (422), (511), and (440) crystal planes of the Fe_3O_4 support, respectively. The diffraction peaks for the supported metal particles were too weak to analyze due to the strong diffraction signals of the support.

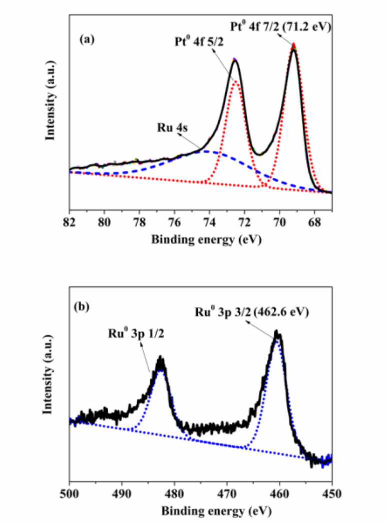

Figure 2. XPS of platinum (a) and ruthenium (b) in Ru-Pt/Fe_3O_4.

Pt and Ru nanoparticles with the inter-fringe distances of 0.227 and 0.206 nm, respectively, were observed in the HRTEM images of as-prepared Ru-Pt/Fe_3O_4 (Figure 3). EDX mapping measurements on Ru-Pt/Fe_3O_4 revealed that some Pt nanoparticles contacted Ru nanoparticles in this catalyst (Figure 4b-d). Based on the aforementioned characterization results, we can conclude that the prepared bi-metallic catalyst Ru-Pt/Fe_3O_4 is composed of nanoparticles of Pt and Ru deposited on Fe_3O_4.

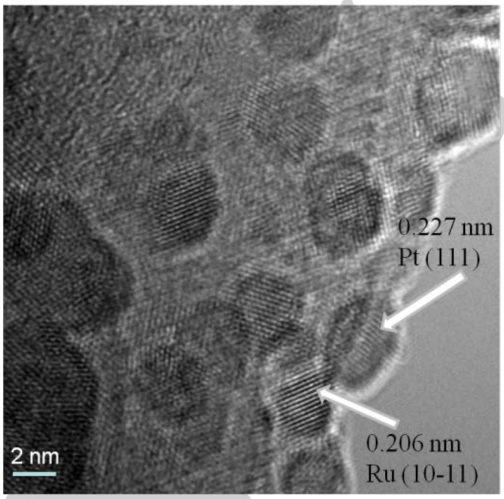

Figure 3. HRTEM image of Ru-Pt/Fe_3O_4.

The catalytic properties for CCMC over Ru-Pt/Fe_3O_4 under different temperatures are listed in Table 1. It was surprise to us that at 40 °C, Ru-Pt/Fe_3O_4 could catalyze CCMC to produce alcohols (C_1-C_6) and higher hydrocarbons (C_2-C_6). The selectivity for alcohols reached as high as 77.1%, while that for methane was only 3.4% (carbon based). In the products of the reaction at 60 °C, the selectivity for alcohols was 41.2%, and that for MCA was 9.1%, respectively. Moreover, the selectivity for higher hydrocarbons was 44.2%, and that for C_2^+ compounds reached 61.9%. When the reaction was performed at 80 °C, C_1-C_8 alcohols and C_1-C_8 hydrocarbons were produced at a CO_2 conversion of 11.4%, and selectivity for MCA and higher hydrocarbons were 6.2% and 55.5%, respectively. At 130 °C, Ru-Pt/Fe_3O_4 could catalyze CCMC to produce alcohols (C_1-C_8) and higher hydrocarbons (C_2-C_8), but the selectivity for methane reached 60.1%, which could be ascribed to the relative high H termination reaction rate at high temperature. CO was not detected in the gaseous mixture recovered from the reaction system, suggesting that the concentration of CO in the mixture was less than the detection limit of the gas chromatography (~60 ppm). The distributions of produced alcohols under different temperatures are shown in Figure 5. It should be mentioned that over a PtRu/Fe_2O_3 catalyst prepared according to the previously reported method [21], only methanol and ethanol were detected in the hydrogenation of CO_2 at 130 °C (Supporting Information Table S1).

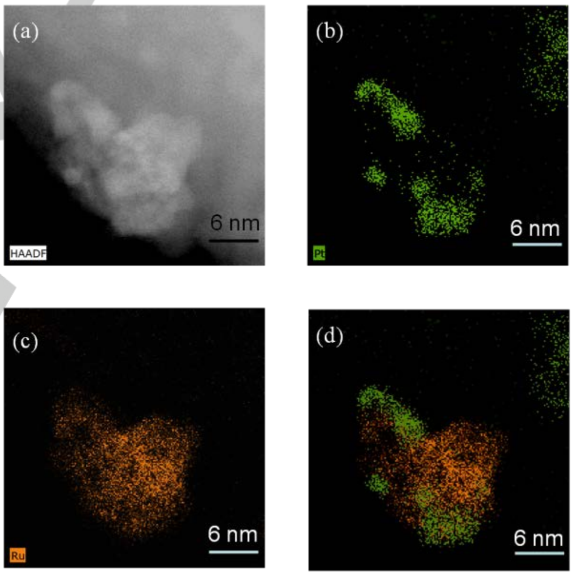

Figure 4. HAADF-STEM image of Ru-Pt/Fe_3O_4 (a), EDX elemental mapping of platinum (b) and ruthenium (c) in the same area, and merged image of b and c (d).

The stability of Ru-Pt/Fe_3O_4 in the hydrogenation of CO_2 was tested at 80 ºC by catalyst recycling test. Over the fresh catalyst, the conversion of CO_2 in 6 days was 11.5%, and the selectivity for higher hydrocarbons and alcohols were 55.5% and 14.9%, respectively. Over the recovered catalysts, the conversion of CO_2 in 6 days (10.3%) decreased by 10%, and the selectivity for higher hydrocarbons and alcohols (53.5 % and 12.5%, respectively) declined slightly, implying a good stability of the catalyst under these conditions.

Table 1. Catalytic performance over Ru-Pt/Fe_3O_4 in CCMC under different temperatures.

T (ºC)	Sel (%)[a]					Conv (%)[a]
	CH_4	RH[b]	Alcohol	Alcohol (C_2^+)	MCA[c]	
40	3.4	19.5	77.1	24.8	4.5	2.0
60	14.6	44.2	41.2	17.7	9.1	2.1
80	29.6	55.5	14.9	9.5	6.2	11.5
130	60.1	36.3	3.6	2.2	0.9	15.6

Reaction conditions: water, 30 mL; initial pressure, 3.0 MPa (H_2/CO_2=3:1); Mass of catalyst in reactions at 40, 60, 80 ºC was 0.50 g, and that in reaction at 130 ºC was 0.15 g. Time for reaction at 40, 60, and 80 ºC was 6 days, and that for reaction at 130 ºC was 0.33 days. [a] Selectivity (Sel) and conversion (Conv) (%) calculations were based on the moles of carbon. [b] RH represents higher hydrocarbons (C_2^+). [c] MCA produced at 40 and 60 ºC were C_3-C_6 alcohols, while those produced at 80 and 130 ºC were C_3-C_8 alcohols.

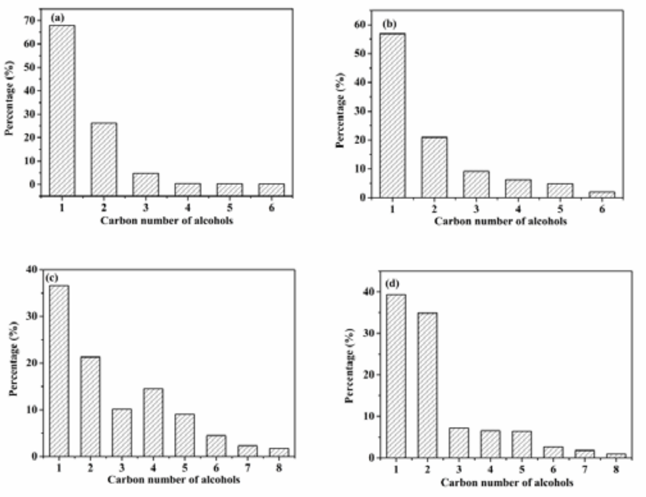

Figure 5. Distribution of the produced alcohols over Ru-Pt/Fe_3O_4 by CCMC at 40 °C (a), 60 °C (b), 80 °C (c) and 130 °C (d).

It was reported that CO insertion into a metal-alkyl bond, followed by reduction of the formed intermediates with H_2 over some catalysts at high temperatures, could lead to the formation of C_2^+ alcohols in the conversion of CO_2 [20, 22, 30], and the alkyl could form through the hydrogenation of CO followed by carbon-carbon coupling [20]. However, it was found that MCA could form by hydrolysis of alkyl over the present catalyst in our isotope tracer experiments, which was different from the previously reported CO insertion pathway. When CCMC over Ru-Pt/Fe_3O_4 was conducted in O^{18} labeled water (5 mL, purity: 97%, isotope tracer experiment) at 80 °C (See the experimental section), the intensity of ion peak corresponding to $[CH_2O^{18}H]^+$ with a m/z value of 33 in the mass spectrum of formed MCA dramatically enhanced. The isotope ratio of O^{18} to O^{16} in the propanol and butanol produced in O^{18} labeled water was 1.4 and 1.6, respectively, while those in propanol and butanol produced in non-labeled water were less than 0.1 (Supporting Information Figure S2). In the mass spectrum of carbon dioxide collected from the isotope tracer experiment reaction system, the ion peaks with m/z values of 44, 46, and 48, corresponding to $[^{16}O{=}C{=}O^{16}]^{\cdot+}$, $[^{18}O{=}C{=}O^{16}]^{\cdot+}$, and $[^{18}O{=}C{=}O^{18}]^{\cdot+}$, respectively, were clearly observed (Supporting Information Figure S3). The relative intensities of the ion peaks for $[^{16}O{=}C{=}O^{16}]^{\cdot+}$, $[^{18}O{=}C{=}O^{16}]^{\cdot+}$, and $[^{18}O{=}C{=}O^{18}]^{\cdot+}$ were 65, 100, and 54, respectively. The transfer of O^{18} from H_2O^{18} to CO_2 could be attributed to the water gas shift reaction ($CO + H_2O = CO_2 + H_2$). If MCA in this experiment formed via the CO insertion pathway exclusively, the ratio of O^{18} to O^{16} in MCA would be the same as that of CO^{18} to CO^{16} derived from the hydrogenation of carbon dioxide in the reaction system, and the isotope ratio of O^{18} to O^{16} in the produced MCA would be no more than 0.9 as calculated from the aforementioned relative peak intensities [(54+100×0.5)/(65+100×0.5)]. However, the isotope ratio of O^{18} to O^{16} in propanol (1.4) and butanol (1.6) formed in O^{18} labeled water was much higher than 0.9, indicating that MCA could form by the hydrolysis of alkyl over Ru-Pt/Fe_3O_4. The new reaction pathway for the formation of MCA over Ru-Pt/Fe_3O_4 is shown in Figure 6.

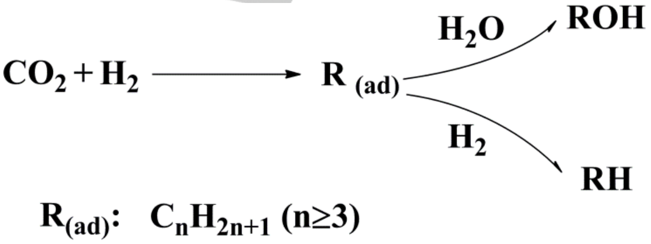

Figure 6. Reaction pathway for MCA formation based on alkyl hydrolysis over Ru-Pt/Fe_3O_4.

Hydrogenation of CO_2 over Ru-Pt/Fe_3O_4 in O^{18} labeled water was also conducted at 130 ºC that is close to the reaction temperature (140 ºC) in previous reports [22]. After 8 hours of reaction, the ratios of O^{18} to O^{16} in the produced butanol and pentanol were 1.7 and 1.4, respectively, which were much larger than that in CO_2 (0.8) collected from the reaction system (Supporting Information Figure S4, 5). This result indicated that multi-carbon alcohols could also form by catalytic hydrolysis of alkyl over Ru-Pt/Fe_3O_4 at 130 ºC.

In the mass spectrum of water collected from the isotope tracer experiment reaction system, the ion peaks with m/z values of 18 and 20 corresponded to $[H_2O^{16}]^{\cdot+}$ and $[H_2O^{18}]^{\cdot+}$, respectively. The isotope ratio of O^{18} to O^{16} in water declined to 2.1 after reaction, which should be mainly derived from the formation of H_2O^{16} in the hydrogenation of CO_2 (Supporting Information Figure S6). The isotope ratio of O^{18} to O^{16} in propanol (1.4) and butanol (1.6) formed in O^{18} labeled water was lower than that in water after reaction (2.1), implying that a part of O in MCA came from CO_2 or Fe_3O_4.

In order to further understand the formation mechanism of MCA through the reactions of CO_2, H_2, and H_2O over Ru-Pt/Fe_3O_4, control experiments were carried out. Ru-Pt/Fe_3O_4, propene, CO_2, and water were charged in an autoclave which was kept at 130 °C for 8 h to verify if propanol could form by hydrolysis of propene over the Ru-Pt/Fe_3O_4 catalyst (see the Experimental Section for details). Propanol was not detected in the reaction mixture after the treatment, implying that over the present catalyst MCA formed by the hydrolysis of alkyl, rather than alkene.

Moreover, a Pt//Fe_3O_4 catalyst containing 1.8% of Pt and a Ru/Fe_3O_4 catalyst containing 3.6 % of Ru were prepared by the methods reported in this work in the absence of Ru and Pt, respectively. Hydrogenation of CO_2 was performed over Pt/Fe_3O_4 and Ru/Fe_3O_4 in 3 mL of O^{18} labeled water at 80 °C for 6 days, respectively. After the experiments, the ratios of O^{18} to O^{16} in carbon dioxide collected from the reaction systems of Pt/Fe_3O_4 and Ru/Fe_3O_4 were measured to be 1.2 and 1.1, respectively (Supporting Information, Figure S7, 8). The transfer of O^{18} from H_2O^{18} to CO_2 in H_2 over Pt/Fe_3O_4 or Ru/Fe_3O_4 indicated that either Pt or Ru nanoparticles supported on Fe_3O_4 could catalyze the dissociation of water to form active hydroxyl [31].

Higher hydrocarbons (C_2-C_8) were detected in the products of hydrogenation of CO_2 over Ru/Fe_3O_4 in 30 mL of water at 80 °C (Supporting Information, Table S1), while MCA was not detected. This result revealed that Fe_3O_4 supported Ru nanoparticles could catalyze carbon-carbon coupling reaction to form long-chain alkyl, but could not catalyze the coupling of hydroxyl with long-chain alkyl to form MCA. On the other hand, MCA (C_3-C_4) and higher hydrocarbons (C_2-C_5) were detected in the products of hydrogenation of CO_2 over Pt/Fe_3O_4 (Supporting Information, Table S1), implying that Fe_3O_4 supported Pt nanoparticles could catalyze not only the carbon-carbon coupling reaction to form long-chain alkyl, but also the coupling of hydroxyl with long-chain alkyl to form MCA.

In the hydrogenation of CO_2 over Ru/Fe_3O_4 at 80 °C, the average conversion rate of CO_2 was 50 $mmol_{CO2}/mol_{Ru}$/h, and the selectivity for methane was as high as 89.2%. This result revealed that Fe_3O_4 supported Ru nanoparticles could catalyze the hydrogenation of CO_2 to form CH_X* (* represents specie adsorbed on catalysts), and the formed CH_X* tended to react with H* to form methane over the catalyst. However, in the hydrogenation of CO_2 over Pt/Fe_3O_4 under the same reaction conditions, the average conversion rate of CO_2 was only 6.3 $mmol_{CO2}/mol_{Pt}$/h, and the selectivity for methane was 10.6% (Supporting Information, Table S1), implying that Fe_3O_4 supported Pt nanoparticles were not as efficient as Ru/Fe_3O_4 in catalyzing the reduction of CO_2 with H_2 to form CH_X*, but the formed CH* over the catalyst tended to couple with each other to generate long-chain alkyl. The formed long-chain alkyl could terminate with H* or OH* over Fe_3O_4 supported Pt nanoparticles to form higher hydrocarbons or MCA.

A γ-Al_2O_3 supported bimetallic catalyst (Ru-Pt/γ-Al_2O_3) was prepared by a similar method for control experiments. In the products of CO_2 hydrogenation over Ru-Pt/γ-Al_2O_3 at 130 ºC, higher hydrocarbons were detected, but multi-carbon alcohols were not, implying that Fe_3O_4 with oxygen vacancies close to the supported metal nanoparticles [24] also contributed to the catalytic coupling of hydroxyl and alkyl to form multi-carbon alcohols.

Based on these experiments results, we can conclude that in Ru-Pt/Fe_3O_4, Ru nanoparticles played an important role in catalyzing the hydrogenation of CO_2 to form CH_X*, while Pt nanoparticles were mainly responsible for catalyzing the coupling of CH_X* produced on themselves and migrated from attached or adjacent Ru nanoparticles to form long-chain alkyl, and the coupling of long-chain alkyl with hydroxyl to form MCA. The new finding in this work provided a possibility of using CO_2 as a carbon source to produce fine chemicals and liquid fuels at ambient temperature in future by improving the catalytic properties.

In summary, the catalytic conversion of CO_2 and H_2 to MCA and higher hydrocarbons was realized under the very mild conditions over a prepared bimetallic catalyst Ru-Pt/Fe_3O_4 composed of nanoparticles of Pt and Ru on a Fe_3O_4 support. MCA (C_3-C_6) and higher hydrocarbons (C_2-C_6) were produced through the reactions over the catalyst even at 40 °C. A new mechanism of the catalytic conversion of CO_2 to MCA, i.e. the hydrolysis of formed alkyl, was revealed. It was discovered that Ru nanoparticles played an important role in the catalytic hydrogenation of CO_2 to form CH_X species, while Fe_3O_4 supported Pt nanoparticles could catalyze the formation and hydrolysis of long-chain alkyl. Insight into the formation mechanism of MCA over Ru-Pt/Fe_3O_4 provided valuable information for further development of efficient catalysts for the conversion of CO_2 and H_2 to MCA and higher hydrocarbons at mild conditions.

Acknowledgements

The authors express their thanks for the support from the NSFC (grants 21573010 and 21821004), and the Chinese Ministry of Science and Technology (2016YFE0118700).

Keywords: carbon dioxide • multi-carbon compounds • hydrolysis • mild conditions • heterogeneous catalysis

[1] S. Kattel, W. T, Yu, X. F. Yang, B. H. Yan, Y. Q. Huang, W. M. Wan, P. Liu, & J. G. Chen, CO_2 hydrogenation over oxide supported PtCo catalysts: The role of the oxide support in determining the product selectivity. *Angew. Chem. Int. Ed*. **2016,** *55*, 7968-7973.

[2] H. B. Yang, S. F. Hung, S. Liu, K. D. Yuan, S. Miao, L. P. Zhang, X. Huang, H. Y. Wang, W. Z. Cai, R. Chen, J. J. Gao, X. F. Yang, W. Chen, Y. Q. Huang, H. M. Chen, C. M. Li, T. Zhang, & B. Liu, Atomically dispersed Ni (I) as the active site for electrochemical CO_2 reduction. *Nat. Energy.* **2018,** *3*, 140-147.

[3] T. Haas, R. Krause, R. Weber, M. Demler, & G. Schmid, Technical photosynthesis involving CO_2 electrolysis and fermentation. *Nat. Catal.* **2018,** *1*, 32-39 .

[4] M. D. Porosoff, X. F. Yang, J. A. Boscoboinik, & J. G. Chen, Molybdenum carbide as alternative catalysts to precious metals for highly selective reduction of CO_2 to CO. *Angew. Chem. Int. Ed*. **2014**, *53*, 6705-6709.

[5]. J. A. Rodriguez, P. Liu, D. J. Stacchiola, S. D. Senanayake, M. G. White, & J. G. Chen, Hydrogenation of CO_2 to methanol: importance of metal-oxide and metal-carbide interfaces in the activation of CO_2. *ACS Catal*. **2015,** *5*, 6696-6706.

[6] R. Satthawong, N. Koizumi, & C. S Song, P. Prasassarakich, Comparative study on CO_2 hydrogenation to higher hydrocarbons over Fe-based bimetallic catalysts. *Top. Catal*. **2014,** *57*, 588-594.

[7] F. S. Ding, A. F. Zhang, M. Liu, Y. Zuo, K. Y. Li, X. W. Guo, & C. S. Song, CO_2 hydrogenation to hydrocarbons over iron-based catalyst: effects of physiochemical properties of Al_2O_3 supports. *Ind. Eng. Chem. Res*. **2014,** *53*, 17563-17569.

[8] S. Saeidi, N. A. S. Amin, & M. R. Rahimpour, Hydrogenation of CO_2 to value-added products-A review and potential future developments. *J. CO_2. Util.* **2014,** *5*, 66-81.

[9] K. Chang, T. F. Wang, & J. G. Chen, Hydrogenation of CO_2 to methanol over CuCeTiOx catalysts. *Appl. Catal. B: Environ*. **2017,** *206*, 704-711.

[10] F. D. Meylan, V. Moreau, & S. Erkman, CO_2 utilization in the perspective of industrial ecology, an overview. *J. CO_2. Util.* **2015,** *12*, 101-108.

[11] Q. Q. Chen, M. Lv, Z. Y. Tang, H. Wang, W. Wei, & Y. H. Sun, Opportunities of integrated systems with CO_2 utilization technologies

for green fuel and chemicals production in a carbon-constrained society. *J. CO_2. Util*. **2016,** *14*, 1-9.

[12] E. V. Kondratenko, J. Baltrusaitis, G. O. Larrazabal, & J. Perez-Ramirez, Status and perspectives of CO_2 conversion into fuels and chemicals by catalytic, photocatalytic and electrocatalytic processes. *Energy. Environ. Sci.* **2013,** *6*, 3112.

[13] R. W. Dorner, D. R. Hardy, F. W. Williams, & H. D. Willauer, Heterogeneous catalytic CO_2 conversion to value-added hydrocarbons. *Energy. Environ. Sci.* **2010,** *3*, 884-890.

[14] S. A. Mavlyankariev, S. J. Ahlers, V. A. Kondratenko, D. Linke, & E.V. Kondratenko, Effect of support and promoter on activity and selectivity of gold nanoparticles in propanol synthesis from CO_2, C_2H_4, and H_2. *ACS Catal.* **2016,** *6*, 3317−3325.

[15] C. R. Ho, S. Shylesh, & A. T. Bell, Mechanism and kinetics of ethanol coupling to butanol over hydroxyapatite. *ACS Catal.* **2016,** *6,* 939−948.

[16] H. T. Luk, C. Mondelli, D. C. Ferre, J. A. Stewartb, & J. Perez-Ramirez, Status and prospects in higher alcohols synthesis from syngas. *Chem. Soc. Rev.* **2017,** *46,* 1358-1426.

[17] R. Satthawong, N. Koizumi, C. S. Song, & P. Prasassarakich, Bimetallic Fe-Co catalysts for CO_2 hydrogenation to higher hydrocarbons. *J. CO_2. Util.* **2013,** *3-4*, 102-106**.**

[18] J. Wei, Q. J. Ge, R. W. Yao, Z. Y. Wen, C. Y. Fang, L. S. Guo, H. Y. Xu, & J. Sun, Directly converting CO_2 into a gasoline fuel. *Nat. Commun.* **2017,** *8*, 15174.

[19] P. Gao, S. G. Li, X. N. Bu, S. S. Dang, Z. Y. Liu, H. Wang, L. S. Zhong, M. H. Qiu, C. G. Yang, J. Cai, W. Wei, & Y. H. Sun, Direct conversion of CO_2 into liquid fuels with high selectivity over a bifunctional catalyst. *Nat. Chem.* **2017,** *9*, 1019-1024.

[20] S. G. Li, H. J. Guo, C. R. Luo, H. R. Zhang, L. Xiong, X. D. Chen, & L. L. Ma, Effect of iron promoter on structure and performance of K/Cu-Zn catalyst for higher alcohols synthesis from CO_2 hydrogenation. *Catal. Lett*. **2013,** *143*, 345-355.

[21] Z. H. He, Q. L. Qian, Z. F. Zhang, Q. L. Meng, H. C. Zhou, Z. W. Jiang, & B. X. Han, Synthesis of higher alcohols from CO_2 hydrogenation over a PtRu/Fe_2O_3 catalyst under supercritical condition. *Phil. Trans. A.* **2015,** *373*, 0006.

[22] Z. H. He, Q. L. Qian, J. Ma, Q. L. Meng, H. C. Zhou, J. L. Song, Z. M. Liu, & B. X. Han, Water-enhanced synthesis of higher alcohols from CO_2 hydrogenation over a Pt/Co_3O_4 catalyst under milder conditions. *Angew. Chem. Int. Ed*. **2016,** *55*, 737-741.

[23] L. X. Wang, L. Wang, J. Zhang, X. L. Liu, H. Wang, W. Zhang, Q. Yang, J. Y. Ma, X. Dong, S. J. Yoo, J. G. Kim, X. J. Meng, F. S. Xiao, Selective hydrogenation of CO_2 to ethanol over cobalt catalysts. *Angew. Chem. Int. Ed*. **2018,** *57*, 6104-6108.

[24] M. H. Liang, X. D. Wang, H. Q. Liu, H. C. Liu, & Y. Wang, Excellent catalytic properties over nanocomposite catalysts for selective hydrogenation of halonitrobenzenes. *J. Catal.* **2008,** *255*, 335-342.

[25] J. L. Zhang, Y. Wang, H. Ji, Y. G. Wei, N. Z. Wu, B. J. Zuo, & Q. L. Wang, Magnetic nanocomposite catalysts with high activity and selectivity for selective hydrogenation of ortho-chloronitrobenzene. *J. Catal.* **2005,** *229*, 114-118.

[26] B. J. Zuo, Y. Wang, Q. L. Wang, Z. L. Zhang, N. Z. Wu, L. D. Peng, L. L. Gui, X. D. Wang, R. M. Wang, & D. P. Yu, An efficient ruthenium catalyst for selective hydrogenation of ortho-chloronitrobenzene prepared via assembling ruthenium and tin oxide nanoparticles. *J. Catal*. **2004,** *222*, 493-498.

[27] C. Lian, H. Q. Liu, C. Xiao, W. Yang, K. Zhang, Y. Liu, & Y. Wang, Solvent-free selective hydrogenation of chloronitrobenzene to chloroaniline over a robust Pt/Fe_3O_4 catalyst. *Chem. Commun.* **2012,** *48*, 3124-3126.

[28] Y. Wang, J. W. Ren, K. Deng, L. L. Gui, & Y. Q. Tang, Preparation of tractable platinum, rhodium, and ruthenium nanoclusters with small particle size in organic media. *Chem. Mater.* **2000,** *12*, 1622-1627.

[29] C. Lian, Y. L. Yu, K. Zhang, A. Gao, & Y. Wang, Highly efficient Fischer-Tropsch synthesis over an alumina supported ruthenium catalyst, *Catal. Sci. Technol.* **2018,** *8*, 1528-1534.

[30] S. X. Bai, Q. Shao, P. T. Wang, Q. G. Dai, X. Y. Wang, & X. Q. Huang, Highly active and selective hydrogenation of CO_2 to ethanol by ordered Pd-Cu nanoparticles. *J. Am. Chem. Soc.* **2017,** *139*, 6827-6830.

[31] L. L. Lin, W. Zhou, R. Gao, S. Y. Yao, X. Zhang, W. Q. Xu, S. J. Zheng, Z. Jiang, Q. L. Yu, Y. W. Li, C. Shi, X. D. Wen, & D. Ma, Low-temperature hydrogen production from water and methanol using Pt/α-MoC catalysts. *Nature.* **2017,** *544*, 80-83.

Entry for the Table of Contents (Please choose one layout)

Layout 1:

COMMUNICATION

Text for Table of Contents

Catalytic conversion of CO_2 and H_2 to multi-carbon alcohols and higher hydrocarbons at ambient temperature.

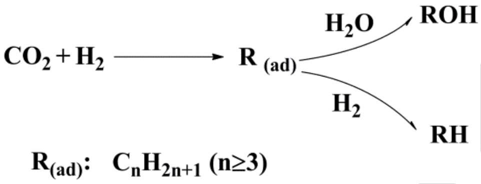

*Yulv Yu, Jin Huang, Yuan Wang**

Page No. – Page No.

Title

Catalytic conversion of CO_2 to value-added products under mild conditions

Layout 2:

COMMUNICATION

((Insert TOC Graphic here))

*Author(s), Corresponding Author(s)**

Page No. – Page No.

Title

Text for Table of Contents